3D generalized nonhyperboloidal moveout approximation[a]

[a]Published in Geophysics, 82, no. 2, C49-C59, (2017)

Yanadet Sripanich[1], *Sergey Fomel*[1], *Alexey Stovas*[2], *and Qi Hao*[2]
[1] *The University of Texas at Austin*
[2] *Norwegian University of Science and Technology (NTNU)*

ABSTRACT

Moveout approximations are commonly used in velocity analysis and time-domain seismic imaging. We revisit the previously proposed generalized nonhyperbolic moveout approximation and develop its extension to the 3D multi-azimuth case. The advantages of the generalized approximation are its high accuracy and its ability to reduce to several other known approximations with particular choices of parameters. The proposed 3D functional form involves seventeen independent parameters instead of five as in the 2D case. These parameters can be defined by zero-offset traveltime attributes and four additional far-offset rays. In our tests, the proposed approximation achieves significantly higher accuracy than previously proposed 3D approximations.

INTRODUCTION

Reflection moveout approximation is an important ingredient for velocity analysis and other time-domain processing techniques (Yilmaz, 2001). As a function of source-receiver offset, the two-way reflection traveltime has the well-known hyperbolic expression, which is exact for plane reflectors in homogeneous isotropic or elliptically anisotropic overburden and approximately valid for small offsets in other cases. This behavior is generally valid for any pure-mode reflections thanks to the source-receiver reciprocity (Thomsen, 2014). At larger offsets, moveout may deviate from hyperbola and behave nonhyperbolically due to the effects of either anisotropy or heterogeneity (Fomel and Grechka, 2001).

In 2D, many extended moveout approximations have been proposed and designed to work with large-offset seismic data. They have led to better stacked sections and successful inversions for anisotropic parameters (e.g. Hake et al., 1984; Castle, 1994; Tsvankin and Thomsen, 1994; Alkhalifah and Tsvankin, 1995; Alkhalifah, 1998; Pech et al., 2003; Fomel, 2004; Taner et al., 2005; Ursin and Stovas, 2006; Blias, 2009; Aleixo and Schleicher, 2010; Golikov and Stovas, 2012; Blias, 2013). Fomel and Stovas (2010) proposed an approximation, which includes five independent parameters that can be

defined from traveltime derivatives at the zero-offset ray and one far-offset ray. This approximation was named *generalized moveout approximation* (GMA) because its functional form reduces to several other known approximation forms with particular choices of parameters and thus, provides a systematic view on the effect of various choices of parameters on the approximation accuracy. Its application to homogeneous TI media was studied by Stovas (2010) and the GMA analog in τ-p domain was developed by Stovas and Fomel (2012). The case of P-SV waves in horizontally layered VTI media was investigated by Hao and Stovas (2015).

The most basic expression for a 3D moveout approximation that works in arbitrary anisotropic heterogeneous media with small offsets can be expressed as the *NMO ellipse* and originates in the second-order Taylor polynomial of traveltime squared around zero offset (Grechka and Tsvankin, 1998; Tsvankin and Grechka, 2011). Several large-offset 3D moveout approximations have also been proposed and applied to seismic velocity analysis in azimuthally anisotropic media (Al-Dajani and Tsvankin, 1998; Al-Dajani et al., 1998; Pech and Tsvankin, 2004; Xu et al., 2005; Vasconcelos and Tsvankin, 2006; Grechka and Pech, 2006; Farra et al., 2016).The general expression for the quartic coefficients was studied by Fomel (1994) and Pech et al. (2003) based on an extension of normal-incident-point theorem.

In this paper, we revisit the 2D generalized nonhyperbolic moveout approximation and develop its natural extension to 3D. We subsequently show that the proposed approximation can be reduced to other known forms with different choices of parameters. Using numerical tests, we show that the 3D GMA can be several orders of magnitude more accurate than previously proposed 3D moveout approximations, at the expense of increasing the number of adjustable parameters. The accuracy and analytical properties of the proposed approximation make it an appropriate choice for 3D moveout approximation in the case of long-offset seismic data.

NONHYPERBOLOIDAL MOVEOUT APPROXIMATION

Let $t(x,y)$ represent the two-way reflection traveltime as a function of the source-receiver offset with components x and y in a given acquisition coordinate frame. We propose the following general functional form of nonhyperboloidal moveout approximation (Sripanich and Fomel, 2015a):

$$t^2(x,y) \approx t_0^2 + W(x,y) + \frac{A(x,y)}{t_0^2 + B(x,y) + \sqrt{t_0^4 + 2t_0^2 B(x,y) + C(x,y)}} \ , \qquad (1)$$

where

$$\begin{aligned} W(x,y) &= W_1 x^2 + W_2 xy + W_3 y^2 \ , \\ A(x,y) &= A_1 x^4 + A_2 x^3 y + A_3 x^2 y^2 + A_4 x y^3 + A_5 y^4 \ , \\ B(x,y) &= B_1 x^2 + B_2 xy + B_3 y^2 \ , \\ C(x,y) &= C_1 x^4 + C_2 x^3 y + C_3 x^2 y^2 + C_4 x y^3 + C_5 y^4 \ , \end{aligned}$$

and t_0 denotes the two-way traveltime at zero offset. The total number of independent parameters in equation 1 is seventeen including t_0, W_i, A_i, B_i, and C_i. A simple algebraic transformation of equation 1 leads to the following expression in polar coordinates:

$$t^2(r,\alpha) \approx t_0^2 + W_r(\alpha)r^2 + \frac{A_r(\alpha)r^4}{t_0^2 + B_r(\alpha)r^2 + \sqrt{t_0^4 + 2t_0^2 B_r(\alpha)r^2 + C_r(\alpha)r^4}} , \tag{2}$$

where

$$\begin{aligned} W_r(\alpha) &= \frac{1}{V_{nmo}^2(\alpha)} = W_1\cos^2\alpha + W_2\cos\alpha\sin\alpha + W_3\sin^2\alpha , \\ A_r(\alpha) &= A_1\cos^4\alpha + A_2\cos^3\alpha\sin\alpha + A_3\cos^2\alpha\sin^2\alpha + \\ &\quad A_4\cos\alpha\sin^3\alpha + A_5\sin^4\alpha , \\ B_r(\alpha) &= B_1\cos^2\alpha + B_2\cos\alpha\sin\alpha + B_3\sin^2\alpha , \\ C_r(\alpha) &= C_1\cos^4\alpha + C_2\cos^3\alpha\sin\alpha + C_3\cos^2\alpha\sin^2\alpha + \\ &\quad C_4\cos\alpha\sin^3\alpha + C_5\sin^4\alpha , \end{aligned}$$

and $r = \sqrt{x^2+y^2}$ represents the absolute offset and α denotes the azimuthal angle from the x-axis. Along a fixed azimuth α, equation 1 reduces to the generalized nonhyperbolic moveout approximation (GMA) of Fomel and Stovas (2010).

Connections with other approximations

1. Setting $A_i = 0$, we can obtain the expression of NMO ellipse from equation 1 (Grechka and Tsvankin, 1998):

$$t^2(x,y) \approx t_0^2 + W(x,y) . \tag{3}$$

2. Setting $C_1 = B_1^2$, $C_2 = 2B_1B_2$, $C_3 = 2B_1B_3 + B_2^2$, $C_4 = 2B_2B_3$, and $C_5 = B_3^2$, we can reduce equation 1 to the following rational approximation, which is reminiscent of several previously proposed approximations (Tsvankin and Thomsen, 1994; Ursin and Stovas, 2006):

$$t^2(x,y) \approx t_0^2 + W(x,y) + \frac{A(x,y)}{2\left(t_0^2 + B(x,y)\right)} . \tag{4}$$

3. Considering equation 2 and a horizontal orthorhombic model with $A_1 = -4\eta_2 W_1^2$, $A_3 = -4\eta_{xy}W_1W_3$, $A_5 = -4\eta_1 W_3^2$, $A_2 = A_4 = 0$, $B_i = 0$, and $C_i = 0$, where η_{xy} is given by (Stovas, 2015)

$$\eta_{xy} = \sqrt{\frac{(1+2\eta_1)(1+2\eta_2)}{1+2\eta_3}} - 1 , \tag{5}$$

equation 2 reduces to the quartic approximation under the acoustic approximation (Alkhalifah, 2003) without the long-offset normalization:

$$\begin{aligned} t^2(r,\alpha) &\approx t_0^2 + W_r(\alpha) r^2 + A_r(\alpha) r^4 \ . \\ &\approx t_0^2 + W_r(\alpha) r^2 - \frac{2}{t_0^2}\left(\eta_2 W_1^2 \cos^4\alpha + \eta_{xy} W_1 W_3 \cos^2\alpha \sin^2\alpha + \eta_1 W_3^2 \sin^4\alpha\right) r^4 \ . \end{aligned} \tag{6}$$

Here, η_1, η_2, and η_3 represent the anellipticity parameters in the planes $[y,z]$, $[x,z]$, and $[x,y]$ respectively (Alkhalifah and Tsvankin, 1995; Alkhalifah, 2003; Stovas, 2015) and their definitions in terms of stiffness coefficients under Voigt notation can be given as follows:

$$\eta_1 = \frac{c_{22}(c_{33}-c_{44})}{2c_{23}(c_{23}+2c_{44})+2c_{33}c_{44}} - \frac{1}{2} \ , \tag{7}$$

$$\eta_2 = \frac{c_{11}(c_{33}-c_{55})}{2c_{13}(c_{13}+2c_{55})+2c_{33}c_{55}} - \frac{1}{2} \ , \tag{8}$$

$$\eta_3 = \frac{c_{22}(c_{11}-c_{66})}{2c_{12}(c_{12}+2c_{66})+2c_{11}c_{66}} - \frac{1}{2} \ . \tag{9}$$

The approximation proposed by Al-Dajani and Tsvankin (1998) and Al-Dajani et al. (1998) has the following additional long-offset normalization factor on the quartic term:

$$1 + A_r^*(\alpha) r^2 \ , \tag{10}$$

where $A_r^*(\alpha) = A_r(\alpha)/\left(1/V_{hor}^2(\alpha) - 1/V_{nmo}^2(\alpha)\right)$, $V_{hor}(\alpha)$ is the phase velocity of P waves in the $[x,y]$ plane as opposed to group velocity. This introduction of the normalization term leads to

$$t^2(r,\alpha) \approx t_0^2 + W_r(\alpha) r^2 + \frac{A_r(\alpha)}{1 + A_r^*(\alpha) r^2} r^4 \ . \tag{11}$$

In the limit of $V_{nmo}^2 \to V_{hor}^2$, $A_r^*(\alpha) \to 0$ and the normalization term becomes equal to one.

4. In an alternative approach to parameterization in an orthorhombic model, we consider the rational approximation in equation 4 with A_i, and B_i normalized by a factor of $1/V_{nmo}^2(\alpha)$. Under the choice of linearized coefficients $A_r(\alpha) = -4\eta(\alpha)/V_{nmo}^4(\alpha)$, and $B_r(\alpha) = (1+2\eta(\alpha))/V_{nmo}^2(\alpha)$, this leads to the moveout approximation of the form proposed by Xu et al. (2005) and Vasconcelos and Tsvankin (2006):

$$t^2(r,\alpha) \approx t_0^2 + W_r(\alpha) r^2 - \frac{2\eta(\alpha)}{V_{nmo}^2(\alpha)\left[t_0^2 V_{nmo}^2(\alpha) + (1+2\eta(\alpha))\, r^2\right]} r^4 \ , \tag{12}$$

where

$$\eta(\alpha) = \eta_2 \cos^2\alpha - \eta_3 \cos^2\alpha \sin^2\alpha + \eta_1 \sin^2\alpha \ . \tag{13}$$

As shown in Appendix A, the moveout approximation in equation 12 can alternatively be derived from generalized quartic coefficients in weakly anisotropic media on the basis of the perturbation theory in combination with the normalization factor in equation 10.

Analogously to the 2D case, we refer to the proposed approximation (equations 1 and 2) as generalized because of its ability to relate to several other known forms.

GENERAL METHOD FOR PARAMETER DEFINITION

To define parameters in equation 1, we propose to use information from the zero-offset ray and four far-offset rays along x-axis, y-axis, $x = y$, and $x = -y$. Following an analogy with the 2D scheme by Fomel and Stovas (2010), we derive some of the coefficient formulas as follows:

Zero-offset ray

The Taylor expansion of equation 1 around the zero offset

$$t^2(x,y) \approx t_0^2 + W(x,y) + \frac{A(x,y)}{2t_0^2} + ... \tag{14}$$

allows for a direct evaluation of nine coefficients: t_0, W_i, and A_i by matching equation 14 with the expansion of the exact traveltime in vector offset.

Sample	c_{11}	c_{22}	c_{33}	c_{44}	c_{55}	c_{66}	c_{12}	c_{23}	c_{13}
HTI	5.06	7.086	7.086	2	2.25	2.25	1.033	3.086	1.033
Layer 1	9	9.84	5.938	2	1.6	2.182	3.6	2.4	2.25
Layer 2	11.7	13.5	9	1.728	1.44	2.246	8.824	5.981	5.159
Layer 3	12.6	13.94	8.9125	2.5	2	2.182	2.7	3.425	3.15

Table 1: Normalized stiffness tensor coefficients (in km^2/s^2) from different anisotropic samples: HTI is from Al-Dajani and Tsvankin (1998), layer 1 is from Schoenberg and Helbig (1997), layer 2 is from Tsvankin (1997), and layer 3 is a modifed sample based on the same fracture model as layer 1.

Finite-offset rays

Suppose that each independent i-th ray corresponds to ray parameters P_{xi} and P_{yi} and arrives at offset X_i and Y_i with reflection traveltime T_i. The i index ranges from 1 to 4 and denotes the associated ray direction of x-axis, y-axis, $x = y$, and $x = -y$ respectively. Substituting moveout approximation 1 into equations $t(X_1, 0) = T_1$ and $dt/dX_1 = P_{x1}$ and solving for B_1 and C_1, we have, from the ray along x-axis ($i = 1$) (Fomel and Stovas, 2010):

$$B_1 = \frac{t_0^2(W_1X_1 - P_{x1}T_1)}{X_1(t_0^2 - T_1^2 + P_{x1}T_1X_1)} + \frac{W_1A_1X_1^2}{T_1^2 - t_0^2 - W_1X_1^2}\ , \tag{15}$$

$$C_1 = \frac{t_0^4(W_1X_1 - P_{x1}T_1)^2}{X_1^2(t_0^2 - T_1^2 + P_{x1}T_1X_1)^2} + \frac{2A_1t_0^2}{t_0^2 - T_1^2 + W_1X_1^2}\ . \tag{16}$$

Analogously, B_3 and C_5 can be found from solving equations $t(0, Y_2) = T_2$ and $dt/dY_2 = P_{y2}$, which is equivalent to replacing X_1, P_{x1}, and W_1 with Y_2, P_{y2}, and W_3 respectively in equations 15 and 16. The remaining coefficients: B_2, C_2, C_3, and C_4 can be solved numerically from the four conditions given below:

$$\frac{\partial t}{\partial y}|_{y=0,\ x=X_1} = P_{y1}\ , \tag{17}$$

$$\frac{\partial t}{\partial x}|_{x=0,\ y=Y_2} = P_{x2}\ , \tag{18}$$

$$t(X_3, X_3) = t(Y_3, Y_3) = T_3\ , \tag{19}$$

$$t(X_4, -X_4) = t(-Y_4, Y_4) = T_4\ . \tag{20}$$

They represents matchings of P_{y1} and P_{x2} along rays in x and y directions and traveltime T_3 and T_4 along rays in $x = y$ and $x = -y$ directions. Provided the above information from the zero-offset ray and four finite-offset rays, we can define the remaining parameters appearing in the proposed moveout approximation (equation 1) in a systematic manner.

ACCURACY TESTS

Homogeneous HTI layer

To test the accuracy of the proposed approximation, we first consider a single horizontal layer of an HTI material over flat reflector with properties given in Table 1 and thickness of 1 km. The accuracy comparison between different approximations is shown in Figure 1with true traveltime computed from ray tracing. The reference rays for the generalized approximation (equation 1) were chosen in terms of different ray parameters P_{xi} and P_{yi}, which then gives X_i, Y_i, and T_i needed to solve for approximation coefficients according to equations 15-20. In this example, the reference rays are associated with $P_{x1} = 0.4$ and and $P_{y1} = 0.0$ along x-axis, at and $P_{x2} = 0.0$ and $P_{y2} = 0.338$ along y-axis, at $P_{x3} = 0.23$ and $P_{y3} = 0.153$ along $x = y$, and at $P_{x4} = 0.23$ and $P_{y4} = -0.153$ along $x = -y$. The proposed approximation shows smaller error than previous approximations (Figure 1c).

Homogeneous orthorhombic layer

For a more complex anisotropic medium, we consider a single horizontal layer of an orthorhombic material (Layer 1) with properties given in Table 1 with 1 km thickness over flat reflector. The accuracy comparison between different approximations is shown in Figure 2. The reference rays for the generalized approximation (equation 1) were shot at $P_{x1} = 0.283$ and and $P_{y1} = 0.0$ along x-axis, at and $P_{x2} = 0.0$ and $P_{y2} = 0.271$ along y-axis, at $P_{x3} = 0.2$ and $P_{y3} = 0.169$ along $x = y$, and at $P_{x4} = 0.2$ and $P_{y4} = -0.169$ along $x = -y$. Note that the approximation by Xu et al. (2005) is

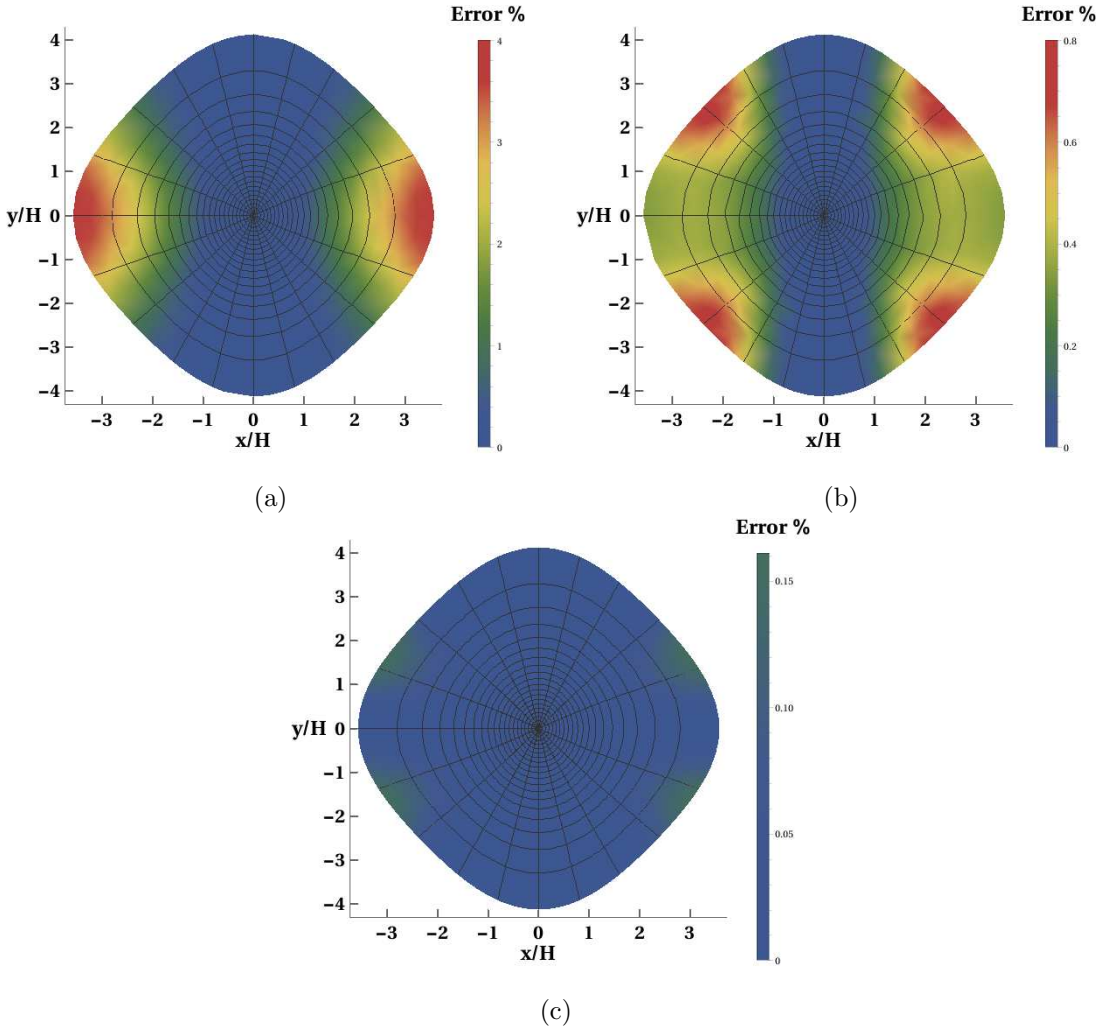

Figure 1: Error plots in the homogeneous HTI layer of a) NMO ellipse b) approximation by Al-Dajani and Tsvankin (1998) (simlar to Al-Dajani et al. (1998)), and c) the proposed approximation. Note that b) and c) are plotted under the same color scale and H denotes the reflector depth.

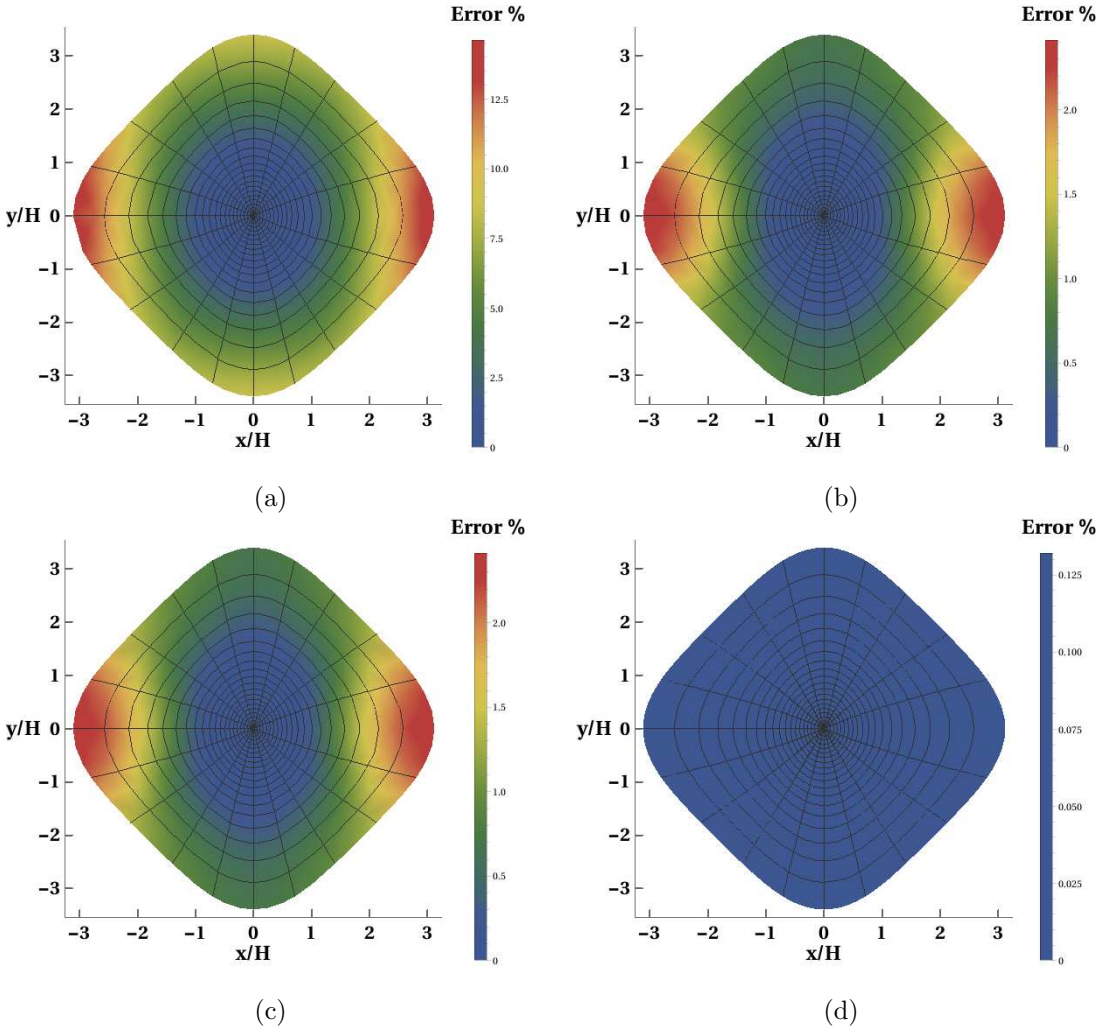

Figure 2: Error plots in the homogeneous orthorhombic layer (Layer 1) of a) NMO ellipse b) approximation by Al-Dajani et al. (1998) c) approximation by Xu et al. (2005), and d) the proposed approximation. Note that b), c), and d) are plotted under the same color scale and H denotes the reflector depth.

a simplified version of that by Al-Dajani et al. (1998) and therefore, produces almost identical results with only a small difference (Figures 2b and 2c). The proposed approximation shows an error, which is several orders of magnitude smaller than that of previous approximations (Figure 2d).

Homogeneous orthorhombic layer with azimuthal rotation

Figure 3 shows the relative error plots of several approximations in a similar homogeneous orthorhombic model as in the previous example but with additional 30 ° azimuthal rotation with respect to the global coordinates. Assuming the rotation azimuth is known, the approximations by Al-Dajani et al. (1998) and Xu et al. (2005) behave largely similar to the original case with the error plots rotated (Figures 3b and 3c). The proposed approximation is implemented based on the global coordinate system regardless of the azimuthal orientation of the orthorhombic symmetry plane and leads to a significantly more accurate result (Figure 3d). The reference rays were shot at $P_{x1} = 0.289$ and $P_{y1} = 0.004$ along x-axis, at $P_{x2} = 0.032$ and $P_{y2} = 0.282$ along y-axis, at $P_{x3} = 0.2$ and $P_{y3} = 0.206$ along $x = y$, and at $P_{x4} = 0.2$ and $P_{y4} = -0.163$ along $x = -y$.

Layered orthorhombic model

We also test the accuracy of the proposed approximation in a three-layer orthorhombic model over flat reflector with parameters (Layer 1-3) listed in Table 1. The thicknesses of the three layers are 0.25, 0.45, and 0.3 km respectively. For previously proposed approximations, the effective coefficients are calculated, as the original authors suggested, by the VTI averaging relationship (Hake et al., 1984; Tsvankin and Thomsen, 1994). The reference rays for the proposed approximation (equation 1) were shot at $P_{x1} = 0.254$ and $P_{y1} = 0.0$ along x-axis, at $P_{x2} = 0$ and $P_{y2} = 0.24$ along y-axis, at $P_{x3} = 0.195$ and $P_{y3} = 0.166$ along $x = y$, and at $P_{x4} = 0.21$ and $P_{y4} = -0.182$ along $x = -y$. The proposed generalized approximation performs with the highest accuracy (Figure 4).

Layered orthorhombic model with azimuthal rotation in sublayers

For a more complex model, we introduce azimuthal rotation of 50 ° and 30 ° in the middle layer (Layer 2) and the bottom layer (Layer 3) of the three-layer model from the previous example respectively. The angle measurement is done with respect to the top layer. Similarly to before, the effective coefficients for previously proposed approximations are calculated by the VTI averaging relationship. The reference rays for the proposed approximation (equation 1) are shot at $P_{x1} = 0.254$ and $P_{y1} = 0.005$ along x-axis, at $P_{x2} = 0.029$ and $P_{y2} = 0.24$ along y-axis, at $P_{x3} = 0.18$ and $P_{y3} =$

0.198 along $x = y$, and at $P_{x4} = 0.2$ and $P_{y4} = -0.184$ along $x = -y$. The proposed generalized approximation shows again the highest accuracy (Figure 5).

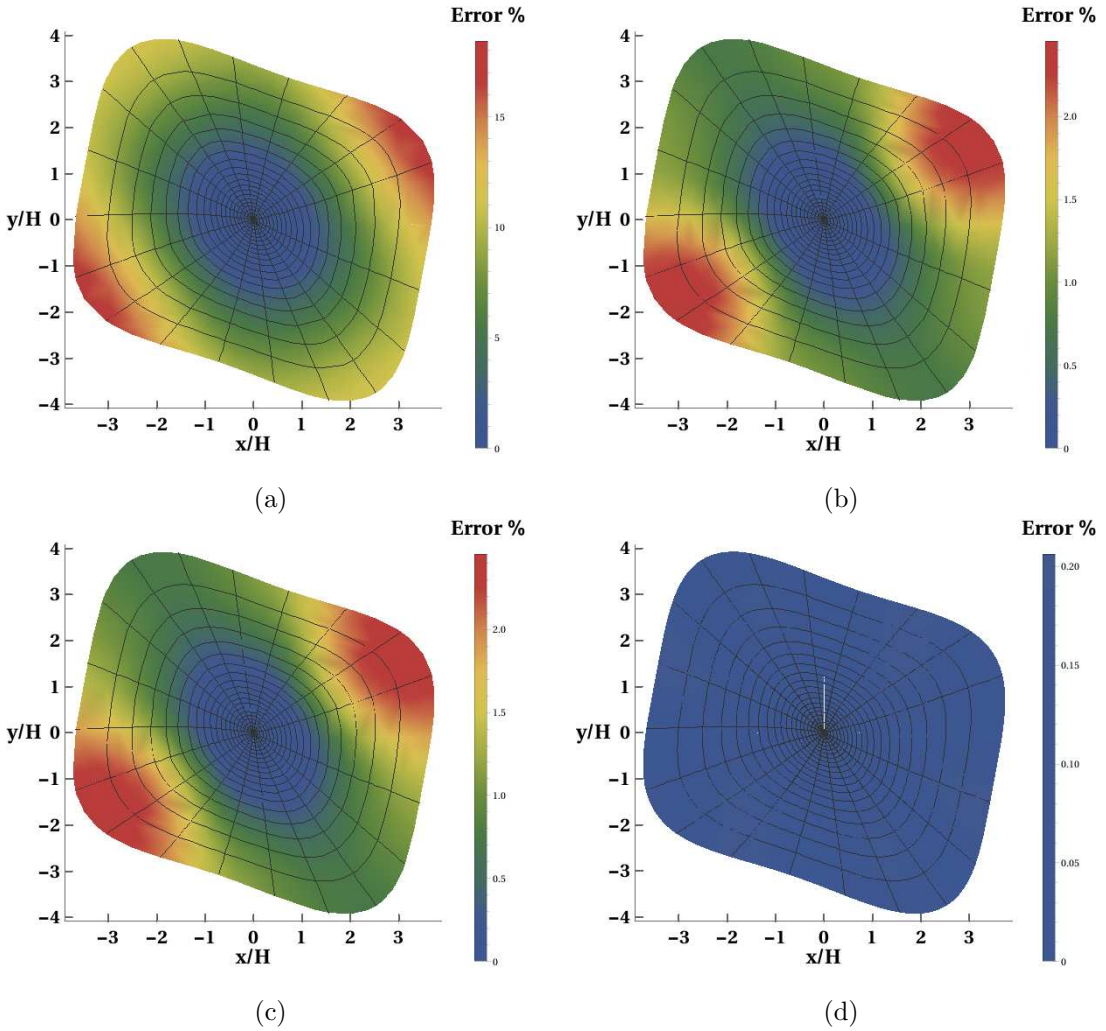

Figure 3: Error plots in the 30° rotated homogeneous orthorhombic layer (Layer 1) of a) NMO ellipse b) approximation by Al-Dajani et al. (1998) c) approximation by Xu et al. (2005) , and d) the proposed approximation. Note that b), c), and d) are plotted under the same color scale and H denotes the reflector depth.

Layered orthorhombic model from SEAM Phase II unconventional model

For a complex numerical test, we create a one-dimensional layered orthorhombic model (Figure 6) by extracting a depth column out of the SEAM Phase II unconventional model (Oristaglio, 2015). We assume no azimuthal rotation in the sublayers. Therefore, this model represents an example of complex layered orthorhombic model with aligned symmetry planes. The reflection traveltimes and offsets can be com-

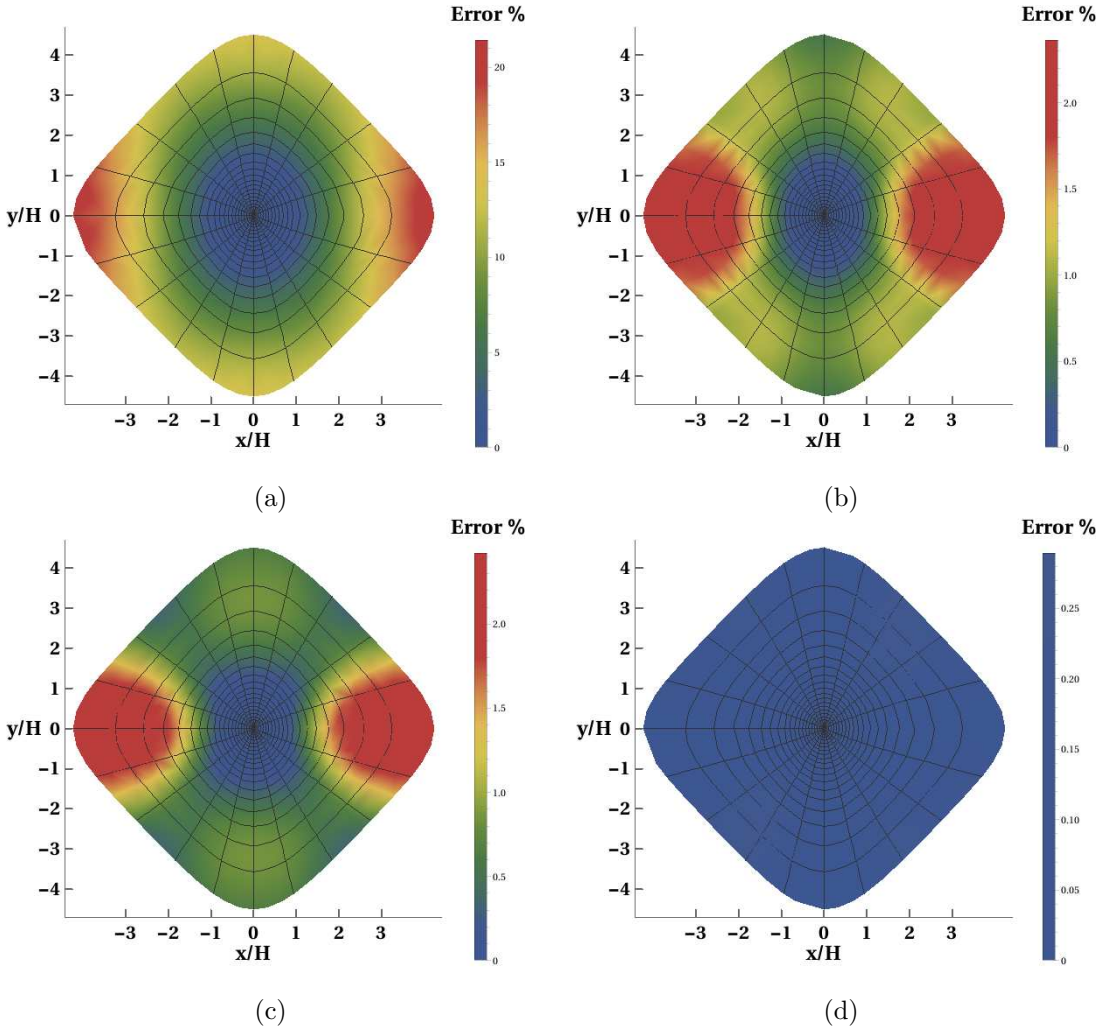

Figure 4: Error plots in the aligned three-layer orthorhombic model of a) NMO ellipse b) approximation by Al-Dajani et al. (1998) c) approximation by Xu et al. (2005), and d) the proposed approximation. Note that b), c), and d) are plotted under the same color scale and H denotes the reflector depth.

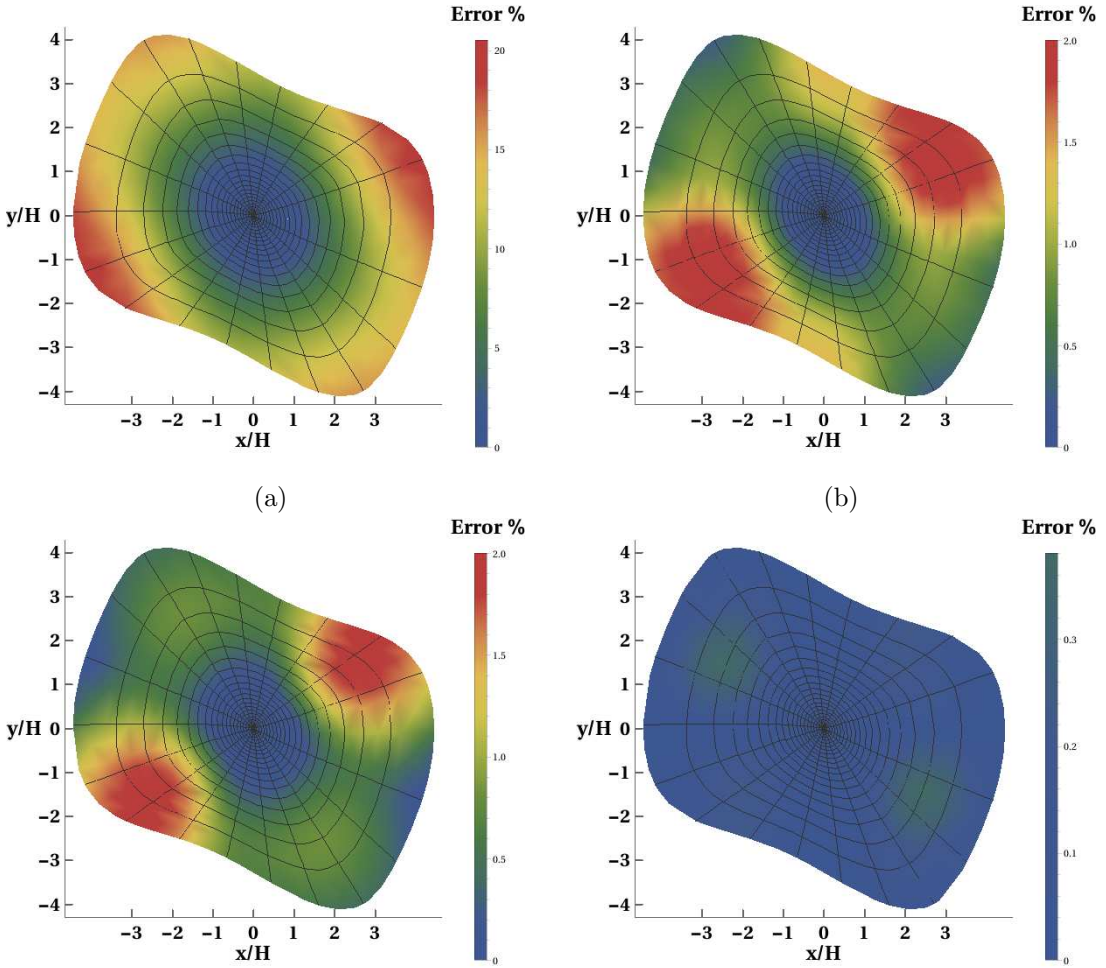

Figure 5: Error plots in the three-layer orthorhombic model with azimuthal rotation of sublayers (50 ° in the middle layer and 30 ° in the bottom layer) of a) NMO ellipse b) approximation by Al-Dajani et al. (1998) c) approximation by Xu et al. (2005), and d) the proposed approximation. Note that b), c), and d) are plotted under the same color scale and H denotes the reflector depth.

puted from ray tracing and are shown in Figure 7. Note that since this is a layered orthorhombic medium with aligned symmetry planes, it is sufficient to show the results only in one quadrant defined by the two slowness components: p_x and p_y as they remain symmetric in all other possible quadrants. Following the similar process as in previous examples, Figure 8 shows a performance comparison of various moveout approximations. The reference rays for the proposed generalized moveout approximation (equation 1) are shot at $P_{x1} = 0.124$ and $P_{y1} = 0.0$ along x-axis, at $P_{x2} = 0.0$ and $P_{y2} = 0.133$ along y-axis, at $P_{x3} = 0.084$ and $P_{y3} = 0.0983$ along $x = y$, and at $P_{x4} = 0.085$ and $P_{y4} = -0.0996$ along $x = -y$. The proposed generalized approximation shows again the highest accuracy with the maximum traveltime error of 6.66 ms and RMS error of 0.083 ms. The maximum traveltime error and RMS error for other approximations are 309.75 ms and 18.86 ms for the NMO ellipse, 66.33 ms and 2.975 ms for the approximation by Al-Dajani et al. (1998), and 110.87 ms and 3.829 ms for the approximation by Xu et al. (2005).

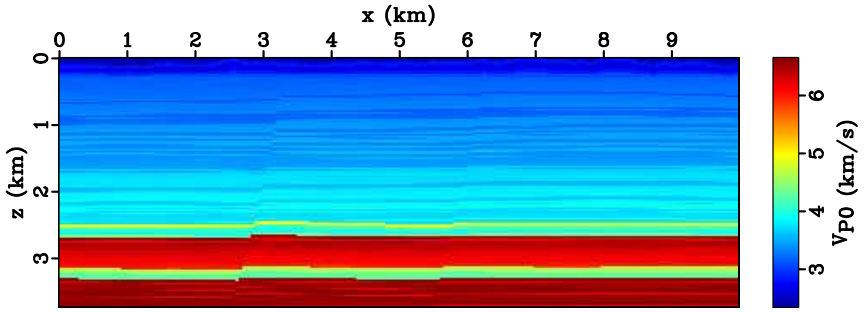

Figure 6: Vertical P-wave velocity in km/s of the SEAM Phase II unconventional model.

DISCUSSION

The choice of scheme for defining coefficient parameters can have an effect on the approximationa ccuracy. We chose to fit nine parameters (t_0, W_i, and A_i) along the zero-offset ray. The remaining eight parameters are divided into six and two fitting equations. The former is from T_1, P_{x1}, and P_{y1} along the x-axis and T_2, P_{x2}, and P_{y2} along the y- axis, while the latter is from T_3 and T_4 along $x = y$ and $x = -y$. Another possible option is to consider T_i and the radial ray parameter $P_{ri}(P_{xi}, P_{yi})$, which would allow two fitting equations from all four directions and make the fitting scheme more symmetric. However, this approach degenerates even in the simple case of a homogeneous orthorhombic layer due to the similarity between $x = y$ and $x = -y$ directions caused by the orthorhombic symmetry. Therefore, we do not propose to use such scheme.

Moreover, the selection of particular rays shot according to the proposed scheme also influences the accuracy level. This issue was originally pointed out by Fomel and Stovas (2010) and has been addressed by Hao and Stovas (2014) in the case of 3D

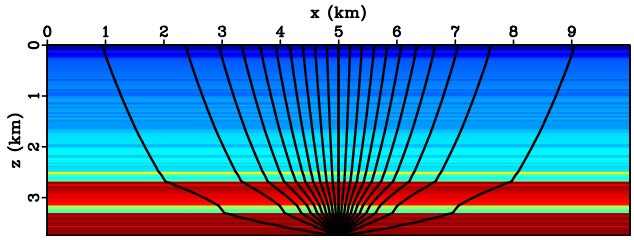

(a)

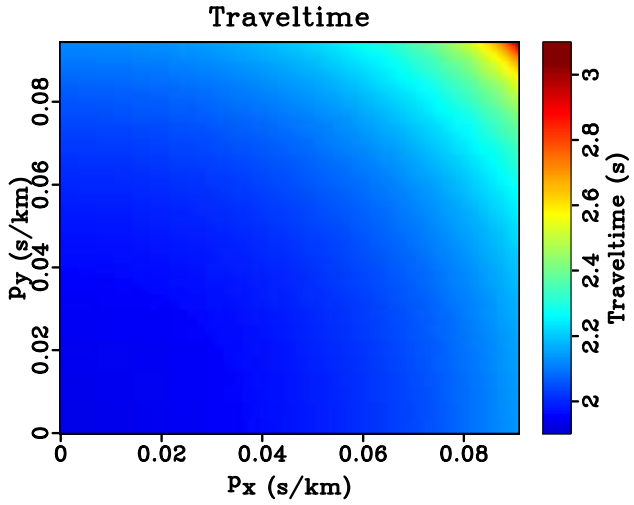

(b)

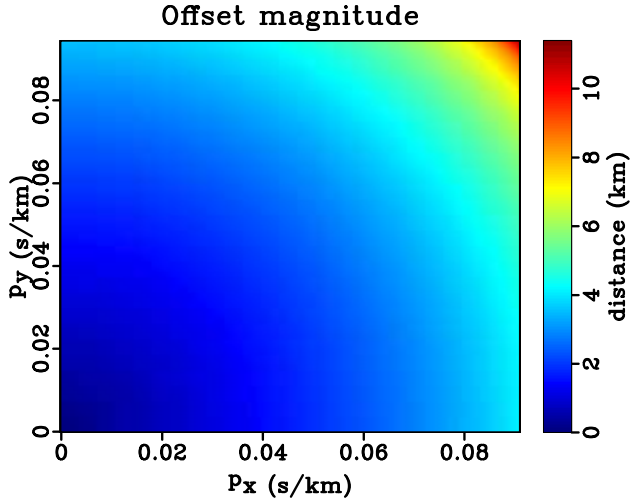

(c)

Figure 7: One-dimensional model construct from the first column of SEAM Phase II unconventional model and a) example reflection rays at constant $p_x = 0.0908$ and varying p_y from 0 to 0.09425. The exact traveltime and the magnitude of offset $r = \sqrt{x^2 + y^2}$ are shown in b) and c) for increasing values of slowness components p_x and p_y.

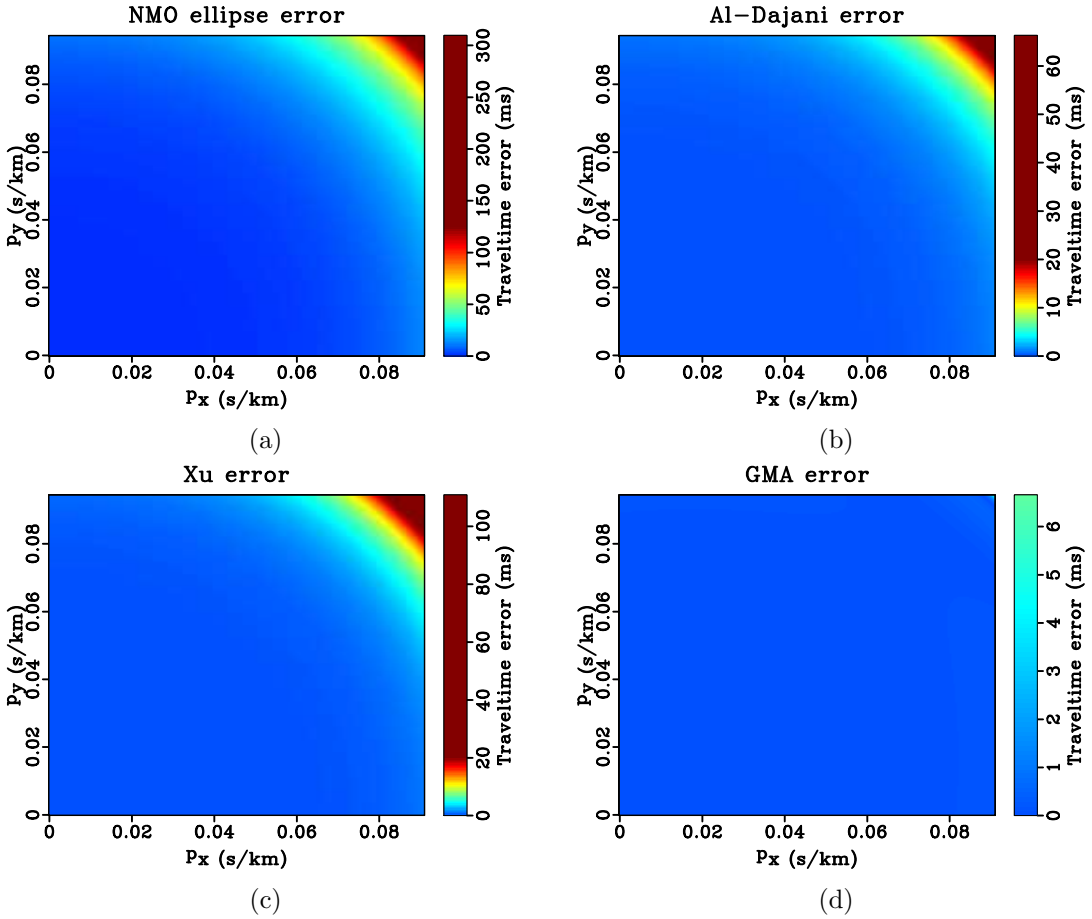

Figure 8: Error plots in the one-dimensional layered orthorhombic model from of SEAM Phase II unconventional model a) NMO ellipse b) approximation by Al-Dajani et al. (1998) c) approximation by Xu et al. (2005), and d) the proposed approximation. Note that a) is plotted with 120 ms clipping, whereas, b), c), and d) are plotted under the same color scale with 25 ms clipping. The scale bars show the total range of errors for different approximations. The proposed approximation achieves the highest accuracy with the maximum traveltime error of 6.66 ms and RMS error of 0.083 ms.

HTI media. In our experiments, we observe that given the four rays at sufficiently far offsets, one can expect the proposed approximation to perform with sufficiently high accuracy for practical purposes with smaller errors closer to the chosen reference offsets.

Analogously to the 2D GMA of Fomel and Stovas (2010), the proposed approximation assumes that the traveltime at infinite offset behaves quadratically as

$$t^2(x,y) \approx T_\infty^2 + P_{x_\infty}^2 x^2 + P_{xy_\infty}^2 xy + P_{y_\infty}^2 y^2 \ , \tag{21}$$

and there are no linear terms present. This might introduce some errors in a special case of having an anomalously high-velocity sublayer in a layered medium (Blias, 2013; Ravve and Koren, 2016). In our approximation, we choose not to complicate the functional form by introducing more parameters to deal wiht this issue.

Even though the required number of parameters for the proposed approximation (seventeen) is high, this number is necessary for an accurate handling of anisotropy with complication from possible azimuthal rotation of the subsurface in 3D. Although other previously proposed approximations require fewer parameters, they may not produce equally accurate results. Figure 9 shows the results approximation of Xu et al. (2005) for the two models from last section, when 20% error is introduced in known azimuthal rotation. We can observe a significant decrease in accuracy especially in the layered case.

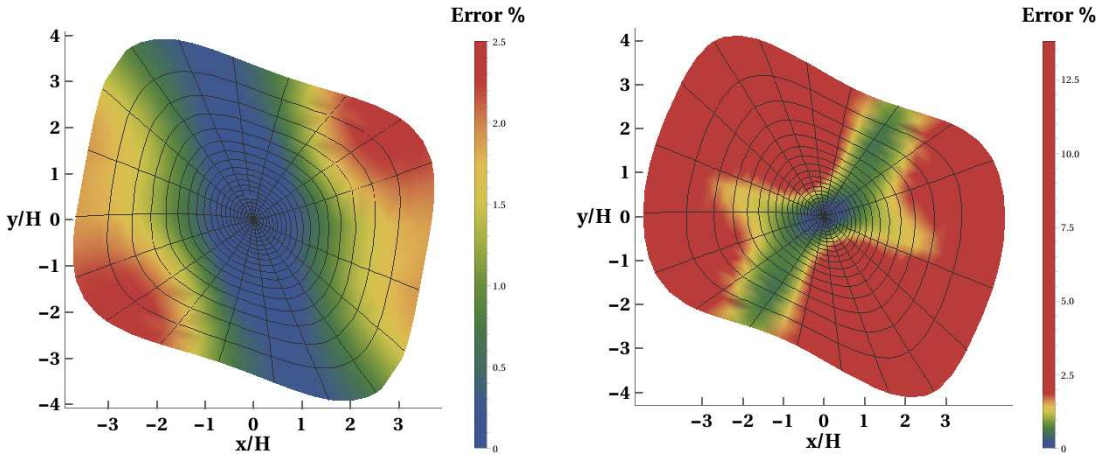

(a) (b)

Figure 9: Error plots of the approximation by Xu et al. (2005) in a) the rotated homogeneous orthorhombic layer (Layer 1) and in b) the three-layer orthorhombic model with azimuthal rotation in sublayers plotted under similar color scales as the originals when 20% error is introduced in known azimuthal angles. One can observe significantly higher errors compared with the original ones in Figures 3c and 5c.

In the case of a single orthorhombic layer, the moveout approximation proposed in our earlier work (Sripanich and Fomel, 2015b), while requiring only six parameters,

exhibits the same level of accuracy as the generalized approximation (Figure 10a). This indicates that the additional nonzero parameters in equation 1 can be captured by the relationship between anelliptic parameters in each symmetry plane (Sripanich and Fomel, 2015b; Sripanich et al., 2016). However, this approach may not be sufficiently accurate in a layered model (Figure 10b).

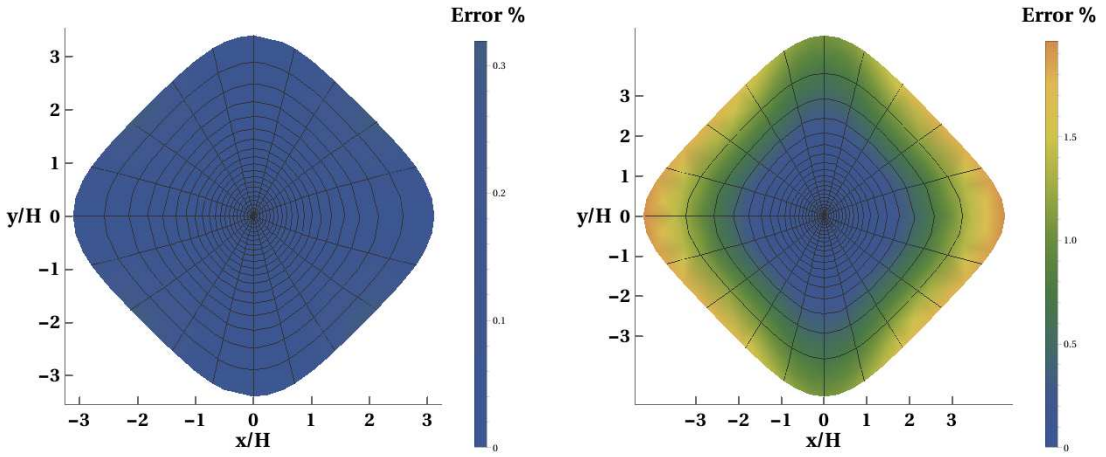

(a) (b)

Figure 10: Error plots of the approximation by Sripanich and Fomel (2015b) in a) the homogeneous orthorhombic layer (Layer 1) and in b) the aligned three-layer orthorhombic model.

Provided that a reflection event can be accurately defined in a gather, the proposed 3D moveout approximation is suitable for anisotropic parameter estimation. One possible method for this application to real seismic data is time-warping (Burnett and Fomel, 2009; Casasanta and Fomel, 2011; Casasanta, 2011), which uses overdetermined least-squares parameter inversion based on local slope estimation and non-physical flattening by predictive painting (Fomel, 2010). This method enables in principles an estimation of all seventeen effective parameters in equation 1, which can then be inverted for interval values in a layer-stripping fashion (Sripanich and Fomel, 2016). In the presence of lateral heterogeneity, the results from such global inversion can be used as a initial model for more sophisticated inversion techniques.

CONCLUSIONS

We have introduced an extension of the generalized moveout approximation to 3D. The proposed approximation, similarly to its 2D analog, reduces to several known functional forms with particular choices of parameters. The approximation requires seventeen parameters, which are uniquely defined by zero-offset computations and four addtional finite-offset rays. Our numerical tests show that, in comparison with other known 3D moveout approximations, the proposed approximation produces results with superior accuracy, which is not surprising given the larger number of ad-

justable parameters. Its advantage becomes more obvious with more complex models. Moreover, the proposed approximation performs well even in the presence of anisotropic axis rotation and multiple layers suggesting that only seventeen parameters are sufficient to describe the reflection traveltime in a model with 3D anisotropic layers. In our experiments, the accuracy can be nearly exact for practical purposes with less than 0.3% in maximum error in both homogeneous and complex layered anisotropic models. The proposed moveout approximation can readily be used for forward reflection traveltime computation or as a basis for inversion for anisotropic parameters from seismic reflection data.

ACKNOWLEDGMENTS

We thank the Assistant Editor, J. Etgen, the Associate Editor and three anonymous reviewers for their constructive comments. We thank the sponsors of the Texas Consortium for Computational Seismology (TCCS) and the Rock Seismic Research Project (ROSE) for financial support. The first author is also grateful to the additional support by the Statoil Fellows Program at the University of Texas at Austin. We are grateful to the Exploration Development Geophysics Education and Research (EDGER) and BP America for their permissions to use SEAM Phase II unconventional model in this study.

APPENDIX A: ALTERNATIVE DERIVATION OF THE MOVEOUT APPROXIMATION IN EQUATION 12

On the basis of perturbation theory for a general horizontal homogeneous weakly anisotropic media, we consider the quartic coefficients in equations 1 and 2 A_i to be (Grechka and Pech, 2006; Farra et al., 2016)

$$\begin{aligned} A_1 &= -\frac{4\eta_2}{V_{\text{ref}}^4} \\ A_2 &= \frac{8(\chi_{13}-\chi_{11})}{V_{\text{ref}}^4} \\ A_3 &= -\frac{4(\eta_1+\eta_2-\eta_3)}{V_{\text{ref}}^4} \\ A_4 &= \frac{8(\chi_{13}-\chi_{12})}{V_{\text{ref}}^4} \\ A_5 &= -\frac{4\eta_1}{V_{\text{ref}}^4}\ , \end{aligned} \tag{A-1}$$

where

$$\chi_{11} = \frac{c_{16}}{V_{\text{ref}}} \quad , \quad \chi_{12} = \frac{c_{26}}{V_{\text{ref}}} \quad , \quad \chi_{13} = \frac{c_{36}+2c_{45}}{V_{\text{ref}}}\ , \tag{A-2}$$

and V_{ref} denotes the P-wave velocity in the chosen isotropic background. These expressions are appropriate for horizontal homogeneous weakly anisotropic media of any symmetry. A more general form form dipping layer is also discussed by Grechka and Pech (2006). In the specific case of orthorhombic media, the general quartic coefficients (equation A-1) can be simplified to

$$A_r(\alpha) = -\frac{4\eta(\alpha)}{V_{\text{ref}}^4} \ , \tag{A-3}$$

where $\eta(\alpha)$ is given in equation 13. Therefore, the resulting moveout approximation takes the form of

$$t^2(r,\alpha) \approx t_0^2 + W_r(\alpha) r^2 - \frac{2\eta(\alpha)}{t_0^2 V_{\text{ref}}^4} r^4 \ . \tag{A-4}$$

Subsequently, by setting

$$V_{\text{ref}}^2 = V_{nmo}^2(\alpha) = (W_r(\alpha))^{-1} \ , \tag{A-5}$$

we obtain the moveout approximation of the form proposed by Xu et al. (2005) and Vasconcelos and Tsvankin (2006):

$$t^2(r,\alpha) \approx t_0^2 + W_r(\alpha) r^2 - \frac{2\eta(\alpha)}{t_0^2 V_{nmo}^4(\alpha)} r^4 \ , \tag{A-6}$$

without the long-offset normalization, which corresponds to the choice of $A_r(\alpha) = -4\eta(\alpha)/V_{nmo}^4(\alpha)$, $B_i = 0$, and $C_i = 0$ from equation 2. The additional long-offset normalization factor can be included based on the same scheme as in equation 10 with

$$A_r^*(\alpha) = \frac{1 + 2\eta(\alpha)}{t_0^2 V_{nmo}^2(\alpha)} \ . \tag{A-7}$$

As a result, we obtain the same expression of the moveout approximation in equation 12 by Xu et al. (2005) in the main text.

REFERENCES

Al-Dajani, A., and I. Tsvankin, 1998, Nonhyperbolic reflection moveout for horizontal transverse isotropy: Geophysics, **63**, no. 5, 1738–1753.

Al-Dajani, A., I. Tsvankin, and M. N. Toksöz, 1998, Non-hyperbolic reflection moveout for azimuthally anisotropic media: 68th Annual International Meeting Expanded Abstracts, Society of Exploration Geophysicists, 1479–1482.

Aleixo, R., and J. Schleicher, 2010, Traveltime approximations for q-P waves in vertical transversely isotropy media: Geophysical Prospecting, **58**, 191–201.

Alkhalifah, T., 1998, Acoustic approximations for processing in transversely isotropic media: Geophysics, **63**, 623–631.

———, 2003, An acoustic wave equation for orthorhombic anisotropy: Geophysics, **68**, 1169–1172.

Alkhalifah, T., and I. Tsvankin, 1995, Velocity analysis for transversely isotropic media: Geophysics, **60**, 1550–1566.

Blias, E., 2009, Long-offset NMO approximation for a layered VTI model: Model study: 79th Annual International Meeting Expanded Abstracts, Society of Exploration Geophysicists, 3745–3748.

———, 2013, High-accuracy two-interval approximation for normal-moveout function in a multi-layered anisotropic model: Geophysical Prospecting, **61**, no. 6, 1229–1237.

Burnett, W., and S. Fomel, 2009, Moveout analysis by time-warping: 79th Annual International Meeting Expanded Abstracts, Society of Exploration Geophysicists, 3710–3714.

Casasanta, L., 2011, NMO-ellipse independent 3D moveout analysis in $\tau - p$ domain: 81tst Annual International Meeting Expanded Abstracts, Society of Exploration Geophysicists, 289–294.

Casasanta, L., and S. Fomel, 2011, Velocity-independent $\tau - p$ moveout in a horizontally-layered VTI medium: Geophysics, **76**, no. 4, U45–U57.

Castle, R. J., 1994, Theory of normal moveout: Geophysics, **59**, 983–999.

Farra, V., I. Pšenčík, and P. Jílek, 2016, Weak-anisotropy moveout approximations for P waves in homogeneous layers of monoclinic or higher anisotropy symmetries: Geophysics, **81**, no. 2, C17–C37.

Fomel, S., 1994, Recurrent formulas for derivatives of a CDP travel-time curve: Russian Geology and Geophysics, **35**, no. 2, 118–126.

———, 2004, On anelliptic approximations for qP velocities in VTI media: Geophysical Prospecting, **52**, 247–259.

———, 2010, Predictive painting of 3-D seismic volumes: Geophysics, **75**, no. 4, A25–A30.

Fomel, S., and V. Grechka, 2001, Nonhyperbolic reflection moveout of P-waves: An overview and comparison of reasons: Technical report, Colorado School of Mines.

Fomel, S., and A. Stovas, 2010, Generalized nonhyperbolic moveout approximation: Geophysics, **75**, no. 2, U9–U18.

Golikov, P., and A. Stovas, 2012, Accuracy comparison of nonhyperbolic moveout approximations for qP-waves in VTI media: Journal of Geophysics and Engineering,

9, 428–432.

Grechka, V., and A. Pech, 2006, Quartic reflection moveout in a weakly anisotropic dipping layer: Geophysics, **71**, no. 1, D1–D13.

Grechka, V., and I. Tsvankin, 1998, 3-D description of normal moveout in anisotropic inhomogeneous media: Geophysics, **63**, no. 3, 1079–1092.

Hake, H., K. Helbig, and C. S. Mesdag, 1984, Three-term Taylor series for $t^2 - x^2$ curves over layered transversely isotropic ground: Geophysical Prospecting, **32**, 828–850.

Hao, Q., and A. Stovas, 2014, Three dimensional generalized nonhyperbolic moveout approximation – Application on a 3D HTI model: Presented at the 76th Annual EAGE Meeting Expanded Abstracts, EAGE.

———, 2015, Generalized moveout approximation for P-SV converted waves in vertically inhomogeneous transversely isotropic media with a vertical symmetry axis: Geophysical Prospecting. (in press).

Oristaglio, M., 2015, Elastic anistropy in SEAM Phase II models: The Leading Edge, **34**, no. 8, 964–970.

Pech, A., V. Grechka, and I. Tsvankin, 2003, Quatic moveout coefficient: 3D description and application to tilted TI media: Geophysics, **68**, no. 5, 1600–1610.

Pech, A., and I. Tsvankin, 2004, Quatic moveout coefficient for a dipping azimuthally anisotropic layer: Geophysics, **69**, no. 3, 699–707.

Ravve, I., and Z. Koren, 2016, Long-offset moveout approximation for VTI elastic layered media: Presented at the 78th Annual EAGE Meeting Expanded Abstracts, EAGE.

Schoenberg, M., and K. Helbig, 1997, Orthorhombic media: Modeling elastic wave behavior in a vertically fractured earth: Geophysics, **62**, 1954–1974.

Sripanich, Y., and S. Fomel, 2015a, 3D generalized nonhyperboloidal moveout approximation: 85th Meeting Expanded Abstracts, Society of Exploration Geophysicists, 5147–5152.

———, 2015b, On anelliptic approximations for qP velocities in transversely isotropic and orthorhombic media: Geophysics, **80**, no. 5, C89–C105.

———, 2016, Theory of interval parameter estimation in layered anisotropic media: Geophysics, **81**, no. 5, C253–C263.

Sripanich, Y., S. Fomel, P. Fowler, A. Stovas, and K. Spikes, 2016, Muir-dellinger parameters for analysis of anisotropic signatures: Presented at the 17th International Workshop on Seismic Anisotropy (IWSA).

Stovas, A., 2010, Generalized moveout approximation for qP-and qSV-waves in a homogeneous transversely isotropic medium: Geophysics, **75**, no. 6, D79–D84.

———, 2015, Azimuthally dependent kinematic properties of orthorhombic media: Geophysics, **80**, no. 6, C107–C122.

Stovas, A., and S. Fomel, 2012, Generalized nonelliptic moveout approximation in $\tau - p$ domain: Geophysics, **77**, no. 2, U23–U30.

Taner, M. T., S. Treitel, and M. Al-Chalabi, 2005, A new traveltime estimation method for horizontal strata: 75th Annual International Meeting Expanded Abstracts, Society of Exploration Geophysicists, 2273–2276.

Thomsen, L., 2014, Understanding Seismic Anisotropy in Exploration and Exploita-

tion, 2 ed.: Society of Exploration Geophysicists and European Association of Geoscientists and Engineers.

Tsvankin, I., 1997, Anisotropic parameters and P-wave velocity for orthorhombic media: Geophysics, **62**, 1292–1309.

Tsvankin, I., and V. Grechka, 2011, Seismology of Azimuthally Anisotropic Media and Seismic Fracture Characterization: Society of Exploration Geophysicists.

Tsvankin, I., and L. Thomsen, 1994, Non-hyperbolic reflection moveout in anisotropic media: Geophysics, **59**, 1290–1304.

Ursin, B., and A. Stovas, 2006, Traveltime approximations for a layered transversely isotropic medium: Geophysics, **71**, no. 2, D23–D33.

Vasconcelos, I., and I. Tsvankin, 2006, Non-hyperbolic moveout inversion of wide-azimuth P-wave data for orthorhombic media: Geophysical Prospecting, **54**, 535–552.

Xu, X., I. Tsvankin, and A. Pech, 2005, Geometrical spreading of P-waves in horizontally layered, azimuthally anisotropic media: Geophysics, **70**, D43–D53.

Yilmaz, O., 2001, Seismic data analysis, 2 ed.: Society of Exploration Geophysicists.